HHS Public Access

Author manuscript

Circ Res. Author manuscript; available in PMC 2020 July 06.

Published in final edited form as:

Circ Res. 2019 October 11; 125(9): 834–846. doi:10.1161/CIRCRESAHA.119.314794.

Yin Yang 1 Suppresses Dilated Cardiomyopathy and Cardiac Fibrosis Through Regulation of *Bmp7* and *Ctgf*

Chia Yee Tan[1,2], **Jing Xuan Wong**[1,2], **Pui Shi Chan**[1,2], **Hansen Tan**[1,2], **Dan Liao**[1,2], **Weiming Chen**[1,2], **Lek Wen Tan**[3], **Matthew Ackers-Johnson**[2,3], **Hiroko Wakimoto**[4], **Jonathan G. Seidman**[4], **Christine E. Seidman**[4], **Ida Gjervold Lunde**[5], **Feng Zhu**[6], **Qidong Hu**[7], **Jinsong Bian**[8], **Jiong-Wei Wang**[2,9,10], **Roger S. Foo**[2,3], **Jianming Jiang**[1,2]

[1]Biochemistry, Yong Loo Lin School of Medicine, National University of Singapore, Singapore 117597;

[2]Cardiovascular Research Institute, National University Health System, Centre for Translational Medicine, Singapore 117599;

[3]Genome Institute of Singapore, A*STAR, Singapore 138672;

[4]Genetics, Harvard Medical School, Boston, MA 02115, USA;

[5]Institute for Experimental Medical Research, Oslo University Hospital and University of Oslo, 0407 Oslo, Norway;

[6]School of Computer, Jiangsu University of Science and Technology, Zhenjiang, P.R China 212003;

[7]Anatomy, Yong Loo Lin School of Medicine, National University of Singapore, Singapore 117594;

[8]Pharmacology, Yong Loo Lin School of Medicine, National University of Singapore, Singapore 117600;

[9]Physiology, Yong Loo Lin School of Medicine, National University of Singapore, Singapore 117593,

[10]Surgery, Yong Loo Lin School of Medicine, National University of Singapore, Singapore 119228

Abstract

Rationale: Pathogenic variations in the lamin gene (*LMNA)* cause familial dilated cardiomyopathy (DCM). *LMNA* insufficiency caused by *LMNA* pathogenic variants is believed to be the basic mechanism underpinning *LMNA*-related DCM.

Objective: To assess whether silencing of cardiac *Lmna* causes DCM and investigate the role of Yin Yang 1 (*Yy1*) in suppressing *Lmna* DCM.

Address correspondence to: Dr. Jianming Jiang, National University of Singapore, Biochemistry, 21 Lower Kent Ridge Road Singapore, Singapore, 119077, Singapore, 66015180, bchjian@nus.edu.sg.

Disclosures

None.

Methods and Results: We developed a *Lmna* DCM mouse model induced by cardiac specific *Lmna* shRNA. Silencing of cardiac *Lmna* induced DCM with associated cardiac fibrosis and inflammation. We demonstrated that upregulation of *Yy1* suppressed *Lmna* DCM and cardiac fibrosis by inducing *Bmp7* expression and preventing upregulation of *Ctgf*. Knockdown of upregulated *Bmp7* attenuated the suppressive effect of *Yy1* on DCM and cardiac fibrosis. However, upregulation of *Bmp7* alone was not sufficient to suppress DCM and cardiac fibrosis. Importantly, upregulation of *Bmp7* together with *Ctgf* silencing significantly suppressed DCM and cardiac fibrosis. Mechanistically, upregulation of *Yy1* regulated *Bmp7* and *Ctgf* reporter activities and modulated *Bmp7* and *Ctgf* gene expression in cardiomyocytes. Downregulation of *Ctgf* inhibited TGFβ/Smad signaling in DCM hearts. Regulation of both *Bmp7* and *Ctgf* further suppressed TGFβ/Smad signaling. In addition, co-modulation of *Bmp7* and *Ctgf* reduced CD3+ T cell numbers in DCM hearts.

Conclusions: Our findings demonstrate that upregulation of *Yy1* or co-modulation of *Bmp7* and *Ctgf* offer novel therapeutic strategies for the treatment of DCM caused by *LMNA* insufficiency.

Graphical Abstract

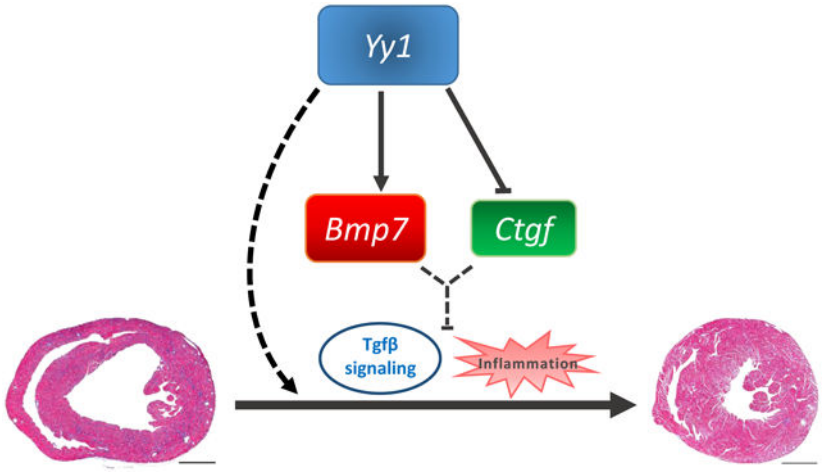

Subject Terms:

Animal Models of Human Disease; Basic Science Research; Fibrosis; Gene Therapy; Inflammation

Keywords

DCM; Cardiac fibrosis; *Yy1*; *Bmp7*; *Ctgf*; cardiomyopathy; gene therapy; transcription factors; fibrosis

Introduction

Dilated cardiomyopathy (DCM) is one of the most common causes of heart failure, an increasingly pandemic condition characterized by impaired cardiac performance and high morbidity and mortality.[1] DCM is defined by the presence of left ventricular (LV) enlargement and contractile dysfunction together with accumulation of interstitial fibrosis.

DCM patients are also at high risk of ventricular arrhythmias and sudden death. As heart failure progresses, treatment options including evidence-based polypharmacy and cardiac resynchronisation therapy may become ineffective, leaving heart transplant as a final resort, but available to very few. Five year mortality after initial diagnosis of heart failure remains approximately 50%. Genetic variations in more than 50 genes have been implicated as causative in DCM[2, 3]. Among them, pathogenic variations in the lamin gene (*LMNA),* encoding A and C- type nuclear lamins (Lamin A/C), are the second most common cause of familial DCM and account for 5–8 % of all cases of autosomal dominant DCM[4]. *LMNA* insufficiency caused by pathogenic variants including missense and nonsense mutations is believed to be the basic mechanism underlying lamin-related DCM. *Lmna* knockout mice (*Lmna* −/−), generated previously, exhibit systemic defects including short lifespan, growth retardation, cardiac defects, muscular dystrophy, neuropathy and lipodystrophy[5–7]. *Lmna* −/− knockout or mutations result in aberrant signaling including autophagy/mTOR, MAPK, WNT/β-catenin and NF-κB signaling pathways[8–12].Modulating activities of p38α, WNT/β-catenin and autophagy/mTOR partially suppresses DCM and/or cardiac fibrosis in *Lmna* animal models, indicating that regulation of aberrant signaling pathways could be beneficial to individuals with *LMNA* related DCM[8, 11, 13].

LMNA is universally expressed in most cell types including cardiomyocytes (CMs) and noncardiomyocytes (non-CMs). It is not known whether silencing of cardiac *LMNA* causes DCM. To circumvent systemic non-cardiac defects or toxicity due to gene targeting, Cre expression or tamoxifen administration, we took advantage of the adeno-associated virus (AAV) system to modulate *Lmna* gene expression in *vivo*[14–16]. Cardiac specific shRNA based on a miRNA backbone and cardiac promoter can be used to reduce gene expression specifically in CMs. Recently, *Lmna* related DCM has been linked to the deregulation of cardiac cell cycle[17, 18]. Additionally, the transcription factor *Yy1* is known to be associated with cell cycle progression[19]. It is not known whether upregulation of *Yy1* could suppress DCM and cardiac fibrosis related to *Lmna* insufficiency. Moreover, it is unknown by what mechanisms and signaling pathways *Yy1* regulates *Lmna* DCM and cardiac fibrosis. Here, we address these major gaps and identify therapeutic candidates that could be translated into treatment for DCM and cardiac fibrosis.

Methods

The authors declare that all supporting data are available within the article and its online supplementary files.

Animal protocols.

All mice were maintained and studied using protocols approved by the Institutional Animal Care and Use Committee (IACUC) of National University of Singapore. Animal work was undertaken in compliance with Singapore National Advisory Committee for Laboratory Animal Research guidelines. Relevant national and institutional guidelines and regulations were consulted before commencement of any animal work. All studies were conducted in male C57BL/6JINV (Jax) mice. Power calculations were performed to estimate sample sizes (error alpha 0.05, power 0.8). For virus injection, 50μl viruses were injected into the thoracic

cavity of 1.5 week old pups via insulin syringe, avoiding the heart and lungs. We selected pups with body weight between 4.5 and 5 g. Overweight or underweight pups were excluded before animal grouping and virus administration. Pups were randomly assigned for injection. For heart harvesting, each mouse was anesthetized with 5% isoflurane and the heart was exposed by opening of the chest. 15% KCl was then injected into the inferior vena cava to achieve asystole at diastole, and the heart was rapidly isolated and flushed with D-PBS injected through the LV to wash out blood while clamping the aorta with Reynolds forceps. Half of the apex was isolated and immersed in RNALater (Qiagen, 76104) at room temperature for RNA extraction, while the other half was snap frozen in liquid nitrogen for protein extraction. The remaining section of the heart was fixed in 4% paraformaldehyde for 24 hours and subsequently embedded in paraffin.

Echocardiogram (Echo) and surface electrocardiogram (ECG).

Mouse cardiac dimensions and function were measured by echocardiography three and/or four weeks after virus transduction (VisualSonics, Vevo 2100, 40 Mhz-550S probe). Investigators were blinded to animal group identities during echo procedure and analysis. All mice were shaved to expose the chest area one day before measurement. During echo, 1.5% isoflurane mixed with oxygen were applied to each mouse, and cine of 300 frames of both B mode and M mode (left parasternal long and short axes) were recorded when heart rate was around 450–500 bpm. Measurements were processed by Vevo®LAB (VisualSonics Inc.). LV tracings were averaged from at least 3 consecutive heart beats of M-mode. LVDD (LV diastolic dimensions), LVWT (LV posterior wall thickness), EF (ejection fraction) and FS (fractional shortening) were obtained from short axis images.

Cell culture and transfection.

HEK293T (ATCC CRL-1573™) cells were cultured at 37 °C with 5% CO2, maintained in DMEM (Hyclone) supplemented with 10 % FBS (Hyclone), 1 mM sodium pyruvate, and 10 μg/ml gentamicin (Invitrogen 15750060). Transfection of shRNA constructs and other plasmids was performed using PEI (Polysciences. Inc, 24765–2) or Lipofectamine 3000 (Invitrogen L3000015) according to manufacturer's instructions.

Recombinant adeno-associated virus 9 (rAAV9) production, purification and titration.

In brief, rAAVs were produced in HEK293T cells by transient triple plasmid transfection, including rAAV viral vector with gene to be delivered, helper plasmids pAdΔF6 and plasmid pAAV2/9 (Penn Vector Core). AAV constructs were propagated using Stbl3 competent cells (Thermo Fisher Scientific, C7373–03). Three days after transfection, viruses were collected from cell pellets and were purified by Optiprep density gradient medium (Sigma, D-1556). After concentration using centrifugal filters (Milipore, UFC910096), viruses were aliquoted and stored at −80°C. For virus titration, forward primer: gataaaagcagtctgggctttcaca and reverse primer: gagcccatataagcccaagctattg were designed to target the rAAV genome-containing particle, cTnT promoter region, and to determine the physical titers by qPCR.

Vector construction

shRNA candidates were designed to target 21 base-pair gene-specific regions (Invitrogen). The miR-155 backbone based shRNA cassette was inserted at the 3 prime end of the AAV-*cTnT-EGFP* vector. *EGFP* was replaced by *Bmp7*, *Yy1 and Ccnd1* for gain of function studies. The sequences of shRNAs and cloning primers are as follows:

Lmna shRNA-1	*agtctcgaatccgcattgaca*
Lmna shRNA-2	*ggctaagaagcagcttcagga*
LacZ shRNA	*aaatcgctgatttgtgtagtc*
Bmp7 shRNA	*ctagtggaacatgacaaagaa*
Ctgf shRNA	*cctgtcaagtttgagctttct*
Ccnd1 shRNA	*cagatgtgaagttcatttcca*
Bmp7-F	*ccggctagcatgcacgtgcgctcgctgcgcg*
Bmp7-R	*ccgggtaccctagtggcagccacaggcccggac*
Yy1-F	*gggcaattgatggcctcgggcgacaccctctacat*
Yy1-R	*gggggtacctcactggttgtttttggctttagcg*
Ccnd1-F	*ccccaattgatggaacaccagctcctgtgctg*
Ccnd1-R	*cccggtacctcagatgtccacatctcgcacgtcg*

Promoter regions (~ 1 kb) of *Bmp7* or *Ctgf* were amplified from C57BL/6JINV (Jax) mouse genomic DNA and cloned into pCAG-*Cherry* (Addgene plasmid # 73978) by replacement of the CAG promoter. *Tgfb1*, *Bmp7* and *Yy1* were amplified from mouse heart cDNA and cloned into pCAGIG (Addgene Plasmid #11159). Promoter cloning primers are as follows:

Bmp7-F	atagctagcaaaaatccaagcctggacctcagta
Bmp7-R	tattctagagagtggatctggctgagtcttcttg
Ctgf-F	ataactagtaaaaatccaagcctggacctcagta
Ctgf-R	tatactagtgagtggatctggctgagtcttcttg

RNAseq library preparation and next generation sequencing.

Total RNA from left ventricular tissue of male mice (n = 2 per group) was extracted to establish RNAseq libraries. RNA samples were pre-treated with Truseq Stranded Total RNA Library Prep kit (Illumina, RS-122–2201) to remove abundant cytoplasmic rRNA. The remaining intact RNA was fragmented using a chemical mix, followed by first- and second-strand cDNA synthesis using random hexamer primers. End-repaired fragments were ligated with a unique Illumina adapter. All individually indexed samples were subsequently pooled together and multiplexed for sequencing. Libraries were sequenced using the Illumina Hiseq 2000 sequencing system and paired-end 101bp reads were generated for analysis. Potential genetic candidates (log2 fold change < -1 or > 1, FDR < 0.05 and log2 CPM ≥ 3.32) were identified from DCM group (*Lmna* shRNA) compared to control group (Ctrl shRNA). Differentially expressed genes were uploaded to Morpheus for Hierarchical clustering and

color-coded heat-map. Canonical pathways were analyzed by Gene Set Enrichment Analysis (GSEA, Broad Institute).

Quantitative real-time PCR (qPCR).

Transcription levels were quantified by qPCR. Total RNA was extracted using Trizol. cDNA was synthesized using Maxima First Strand kit (ThermoFisher, K1641) and qPCR was carried out by KAPA SYBR Fast qPCR Master Mix kit (KAPA Biosystems, KR0389). We used ΔCT to quantify relative expression levels and data were normalized to *Ctcf* expression. All qPCR primers are listed as follows:

Primer	sequence	Primer	sequence
EGFP forward	cgaaggctacgtccaggagc	*Tgfb1* forward	gaaggacctgggttggaagtggatc
EGFP reverse	cgatgttgtggcggatcttg	*Tgfb1* reverse	tgtgttggttgtagagggcaaggac
Nppa forward	tttcaagaacctgctagaccacctg	*Tgfb2* forward	attgctgccttcgccctctttacat
Nppa reverse	gcttttcaagagggcagatctatcg	*Tgfb2* reverse	aggctgaggactttggtgtgttgag
Myh7 forward	agcattctcctgctgtttcctt	*Tgfb3* forward	ccagatacttcgaccggatgagcac
Myh7 reverse	tgagccttggattctcaaacg	*Tgfb3* reverse	tctccattgggctgaaaggtgtgac
Ctcf forward	atgtcacaccttacctttgcctgaa	*Col1a1* forward	gagcctgagtcagcagattgagaac
Ctcf reverse	ccttcctgctgttcttcctcaaaat	*Col1a1* reverse	cctgtctccatgttgcagtagacct
Bmp7 forward	agaatcgctccaagacgccaaagaa	*Col1a2* forward	acccttctcactcctgaaggctcta
Bmp7 reverse	ctctccctcacagtagtaggcagca	*Col1a2* reverse	tatgagttcttcgctggggtgttta
Ctgf forward	acacctaaaatcgccaagcctgtca	*Postn forward*	gccttctcttgatcgtcttctaggc
Ctgf reverse	aatggcaggcacaggtcttgatgaa	*Postn reverse*	cttgaggagtacgacgcagaagaag
Ccnd1 forward	atgagaacaagcagaccatccgcaa	*Yy1 forward*	cggggaataagaagtgggagcagaa
Ccnd1 reverse	cggtagcaggagaggaagttgttgg	*Yy1 reverse*	caggagggagtttcttgcctgtcat

Histological and immunostaining analysis.

Heart samples were fixed in 4% paraformaldehyde for 24 hours, then embedded in paraffin and sectioned at 4 μm intervals. Paraffin samples were further treated with xylene (to remove paraffin) and re-hydrated. Hematoxylin and eosin (HE) was applied to observe myocyte architecture and Masson trichrome (MT) to identify cardiac fibrosis. Quantification of fibrosis was calculated as the blue-stained areas relative to total ventricular area, using ImageJ (NIH). For antigen retrieval of αSMA and CD3, samples were boiled in citrate buffer (pH 6.0) after the rehydration step. The following primary antibodies were used: PCM1 (SIGMA, HPA023374), Lamin A/C (Santa Cruz, sc-376248AF594), αSMA (Abcam, ab32575), CD3 (Agilent, A0452), Arginase-1(Cell Signaling Technology. Inc, 93668), Iba-1 (Wako Laboratory chemicals, 019–19741) and cTnI (Abcam, ab8295). DAPI was used for nuclear staining (ThermoFisher, D1306). Species-specific secondary antibody only controls were used to check for signal specificity. Total positive signals from three completed cross sections were counted for each heart sample by an investigator who was blinded to group identities, and data were normalized to total nucleus number or total ventricular area.

Western blots.

Frozen heart tissues were lysed in cold RIPA buffer with protease inhibitor (Sigma, 4693116001) and were homogenized with prechilled TissueLyser (Qiagen, 25/s, 2mins, 3 cycles) and metal beads. 20 μg of each sample was separated by SDS-page gel (10%) and transferred onto nitrocellulose membranes (0.2 μm, Biorad, 162–0112) for blotting. The blots were probed with a primary antibody followed by a secondary antibody conjugated to horseradish peroxidase. The following primary antibodies were used: phospho-Smad2 (Ser465/Ser467) (Cell Signaling Technology, 18338), Ctgf (Santa Cruz Biotechnology, Inc, sc-365970), Bmp7 (Proteintech Group, Inc 12221–1-AP), Ccnd1 (Abcam, ab16663) and Lamin B1 (Abcam, ab16048). The secondary antibody used was Donkey anti-Rabbit IgG (H +L) Highly Cross-Adsorbed Secondary Antibody, HRP (Thermofisher, A16035). Protein levels on the blots were detected using the enhanced chemiluminescence system (GE Healthcare, RPN2106) according to the manufacturer's instructions. Protein band intensity was quantified using Image J (NIH, 1.52e) and protein levels were normalized to Lamin B1.

Statistical analyses.

Statistical analysis was performed by Prism 7.04 (GraphPad Software, La Jolla, California). Sample distribution was tested for normality using a Shapiro-Wilk normality test. For data that followed a normal Gaussian distribution, P value between two groups was obtained by two-tailed, unpaired T-test with Welch correction, and one-way ANOVA with Tukey's multiple comparisons test was performed for comparison of multiple groups. For data that depart from normality, differences between groups were analyzed by Mann-Whitney test. Quantitative data are shown as mean ± SD.

Results

Cardiac Lmna shRNA induces dilated cardiomyopathy.

We developed a *Lmna* DCM mouse model induced by either of two independent *Lmna* shRNAs delivered specifically to cardiomyocytes by AAV as previously described (Figure 1a, Table 1)[14]. Each *Lmna* shRNA caused impaired cardiac contraction, enlarged left ventricle (LV) heart chamber size and reduced LV wall thickness, coupled with interstitial fibrosis. Immunostaining indicated that most CM nuclei marked by PCM-1 in *Lmna* shRNA hearts had reduced Lamin A/C signal (Figure 1b). Lamin A/C was significantly reduced by ~ 75% in CMs derived from *Lmna* shRNA hearts (Figure 1c). To examine pathways regulated by *Lmna* shRNA, we profiled control and *Lmna* shRNA hearts by RNAseq (Online Figure Ia, b). Hierarchical clustering uncovered genes significantly dysregulated in the *Lmna* shRNA group compared to the control shRNA group. We analyzed this gene list by Gene Set Enrichment Analysis (GSEA, Broad Institute). Top significantly enriched upregulated gene sets identified "Matrisome", "Core Matrisome" and "ECM Glycoproteins" that were common in two independent *Lmna* shRNA groups by canonical pathway analysis. Downregulated gene sets were enriched in "TCA cycle and respiratory electron transport", "respiratory electron transport ATP synthesis" and "Oxidative Phosphorylation". Furthermore, common dysregulated gene sets identified hallmark signature associated with fibrosis and inflammation (Online Figure Ic). The results of pathway analysis were concordant with *Lmna* DCM phenotypes including impaired cardiac performance with

fibrosis/extracellular matrix production (ECM). Consistent with cardiac fibrosis and activation of matrisome/ECM pathways, *Lmna* DCM hearts showed a significant upregulation of phosphorylated Smad2 (p-Smad2) and the myofibroblast marker αSMA (Figure 1d, e). Additionally, *Lmna* DCM was also associated with cardiac inflammation indicated by upregulation of macrophage marker Iba-1 and T cell marker CD3 (Figure 1f, g). The two independent *Lmna* shRNAs both induced similar DCM, cardiac fibrosis and cardiac inflammation, indicating the phenotype is not due to a non-specific effect of shRNA. We selected *Lmna* DCM induced by *Lmna* shRNA-1 for subsequent assessment. Taken together, these results suggest *Lmna* DCM activates TGFβ signaling and induces cardiac fibrosis coupled with inflammation.

Yy1 suppresses Lmna DCM and cardiac fibrosis

To assess whether *Yy1* could suppress *Lmna* DCM, we treated *Lmna* DCM mice with either *Yy1* or *EGFP* delivered by AAV at 1.5 weeks old. Four weeks later, ejection fraction (EF) was assessed by echocardiography. EF of *Lmna* DCM mice treated with *Yy*1 was significantly improved compared to those treated with *EGFP*, suggesting that *Yy1* suppresses DCM induced by *Lmna* insufficiency (Table 2). Importantly, cardiac fibrosis was significantly reduced by *Yy1* in *Lmna* DCM hearts (Figure 2a). Fibrosis markers *Col1a1* and *Col1a2* expression were significantly suppressed by *Yy1* (Figure 2b). Consistent with this data, αSMA-positive myofibroblast numbers were significantly reduced in *Lmna* DCM hearts treated with *Yy1* (Figure 2c).

To assess whether *Yy1* suppresses *Lmna* DCM through regulating the cardiac cell cycle, we constructed an AAV vector co-expressing the *Yy1* gene and *Ccnd1* shRNA (designated as *Yy1-Ccnd1* shRNA). *Ccnd1* is a cell cycle related gene regulated by *Yy1*[20]. Although upregulation of *Ccnd1* by *Yy1* was abolished in the group treated with *Yy1-Ccnd1* shRNA, rescue of cardiac performance and fibrosis was not compromised by the *Ccnd1* shRNA (Online Figure IIa, b, Online Table I). *Col1a1* and *Col1a2* expression remained significantly suppressed by *Yy1-Ccnd1* shRNA (Online Figure IIc). Next we examined whether upregulation of *Ccnd1* could suppress *Lmna* DCM. EF of *Lmna* DCM mice treated with *Ccnd1* was not improved compared to those treated with *EGFP* (Online Table II). Cardiac fibrosis was not affected by upregulation of *Ccnd1* in *Lmna* DCM hearts (Online Figure IId, e, f). Consistent with this, *Col1a1* and *Col1a2* expression were not suppressed upon upregulation of *Ccnd1* (Online Figure IIg).

We therefore hypothesized that other downstream targets of *Yy1,* especially secreted factors, might regulate *Lmna* DCM and cardiac fibrosis. TGFβ/Smad signaling is believed to play a key role in cardiac performance and fibrosis[21]. p-Smad2 was elevated in *Lmna* DCM hearts, and this was significantly reduced ~ 65% by *Yy1*, indicating that TGF-β/Smad signaling is suppressed by *Yy1* (Figure 2d). Although the expression of secreted TGFβ cytokines (*Tgfb1*/*2*/*3*) was not significantly affected by *Yy1*, *Ctgf* (connective tissue growth factor) and *Postn* (periostin) were significantly suppressed by *Yy*1 (Figure 2e). Ctgf and periostin are secreted ECM proteins, which are known to be responsive to TGFβ signaling[22, 23]. A member of the TGF-β superfamily, *Bmp7* is dysregulated in the mouse transverse aortic

constriction (TAC) model and clinical aortic stenosis[24, 25]. Importantly, *Bmp7* was significantly upregulated by ~ 10 fold in *Lmna* DCM hearts treated with *Yy1.*

Bmp7 serves as a key downstream target of Yy1 in suppressing Lmna DCM and cardiac fibrosis

To assess whether *Bmp7* is an important downstream target of *Yy1*, we generated an AAV vector co-expressing the *Yy1* gene and *Bmp7* shRNA (designated as *Yy1-Bmp7* shRNA). We treated *Lmna* DCM mice with AAV expressing *Yy1-Bmp7* shRNA, *Yy1*-Ctrl shRNA or *EGFP*-Ctrl shRNA. Cardiac performance and fibrosis was assessed by echocardiography and histology (Table 3, Figure 3a). Importantly, rescue of cardiac performance and fibrosis was compromised by *Bmp7* reduction, suggesting that *Bmp7* serves as a key downstream target of *Yy1* in suppressing *Lmna* DCM and fibrosis. *Yy1-Bmp7* shRNA significantly abolished upregulation of *Bmp7* and attenuated the downregulation of fibrosis markers *Col1a1* and *Col1a2* compared to *Yy1*-Ctrl shRNA (Figure 3b).

Co-modulation of Bmp7 and Ctgf suppresses Lmna DCM and cardiac fibrosis.

Bmp7 antagonizes fibrogenesis in renal and pulmonary disease[26, 27]. To assess whether upregulation of *Bmp7* is sufficient to suppress *Lmna* DCM and cardiac fibrosis, we treated *Lmna* DCM mice with AAV expressing *Bmp7* (Online Table III, Online Figure IIIa). Unexpectedly, we did not observe a rescue effect of *Bmp7* on cardiac performance and fibrosis in *Lmna* DCM mice, suggesting upregulation of *Bmp7* alone is not sufficient to suppress *Lmna* DCM and cardiac fibrosis (Online Figure IIIb). We deduced that additional factors are required to work together with *Bmp7*. *Ctgf* and *Postn,* the downstream responsive genes of TGFβ, were not affected by upregulation of *Bmp7*, suggesting that upregulation of *Bmp7* does not regulates TGFβ signaling in *Lmna* DCM (Online Figure IIIc). *Ctgf* is highly expressed in CMs and upregulated in response to cardiac injury upon TGF-β stimulation[28, 29]. To assess whether *Ctgf* is involved in suppressing *Lmna* DCM, we reduced *Ctgf* expression in *Lmna* DCM mice by *Ctgf* shRNA. Similar to upregulation of *Bmp7*, downregulation of *Ctgf* did not significantly restore cardiac performance, or reduce fibrosis and related markers in *Lmna* DCM mice (Online Table IV, Online Figure IIIc, IIId). To assess whether modulating both *Bmp7* and *Ctgf* could work cooperatively to suppress *Lmna* DCM and cardiac fibrosis, we generated an AAV vector expressing both the *Bmp7* gene and *Ctgf* shRNA (designated as *Bmp7-Ctgf* shRNA). *Lmna* DCM mice were treated with either *Bmp7-Ctgf* shRNA or *EGFP*-control shRNA. Importantly, *Bmp7-Ctgf* shRNA significantly restored cardiac performance in *Lmna* DCM mice compared to those treated with *EGFP*-control shRNA (Table 4). Cardiac fibrosis was significantly reduced in *Lmna* DCM mice treated with *Bmp7-Ctgf* shRNA (Figure 3c). Furthermore, markers of heart failure and cardiac fibrosis including *Myh7*, *Nppa, Col1a1* and *Col1a2* were also significantly suppressed by *Bmp7-Ctgf* shRNA (Figure 3d). We therefore hypothesize that *Yy1* suppresses *Lmna* DCM through upregulation of a member of the TGF-β superfamily (*Bmp7*) and downregulation of a downstream responsive gene of TGFβ signaling pathway (*Ctgf*).

Upregulation of Yy1 induces Bmp7 and suppresses Ctgf in cardiomyocytes.

Bmp7 was induced, while *Ctgf* was downregulated by upregulation of *Yy1* in *Lmna* DCM mice. To assess whether *Yy1* regulates *Bmp7* and *Ctgf* promoter activity, we cloned *Bmp7* and *Ctgf* reporters harboring the promoter regions of *Bmp7* or *Ctgf* before a *Cherry* reporter gene (Online Figure IVa). When co-transfected with *Bmp7-Cherry* reporter in 293T cells, *Yy1* significantly enhanced the activity of *Bmp7-Cherry* reporter, suggesting *Yy1* can directly regulate *Bmp7* promoter activity (Online Figure IVb). *Yy1* did not modulate the activity of *Ctgf-Cherry* reporter, indicating *Yy1* does not regulate basal promoter activity of *Ctgf* (Online Figure IVc). To assess whether *Yy1* prevents upregulation of *Ctgf* promoter activity, we used *Tgfb1* to activate the *Ctgf-Cherry* reporter. Importantly, the enhanced activity of *Ctgf* reporter following *Tgfb1* treatment was abolished by *Yy1*, suggesting *Yy1* can also regulate the promoter activity of *Ctgf* (Online Figure IVd). To examine whether *Yy1* regulates *Bmp7* and *Ctgf* expression in CMs, we isolated CMs from control, *Lmna* DCM or *Lmna* DCM mice treated with *Yy1* as described (Online Figure IVe)[30]. *Bmp7* expression was reduced in CMs isolated from *Lmna* DCM mice. Upregulation of *Yy1* significantly induced *Bmp7* expression. Conversely, *Ctgf* was significantly induced in CMs isolated from *Lmna* DCM mice, and this upregulation was abolished by *Yy1* (Online Figure IVf).

Bmp7 and Ctgf modulate TGFβ signaling and cardiac inflammation.

To dissect the mechanisms of *Bmp7* and *Ctgf* in suppressing DCM, we compared TGFβ signaling and cardiac inflammation in *Lmna* DCM hearts treated with *Bmp7*, *Ctgf* shRNA or *Bmp7-Ctgf* shRNA. Upregulation of p-Smad2 in *Lmna* DCM hearts was not significantly affected by *Bmp7*, suggesting that upregulation of *Bmp7* does not suppress TGFβ signaling (Figure 4a). p-Smad2 elevation was however significantly reduced ~ 30% by *Ctgf* shRNA (Figure 4b). Similar to the suppressive effect of *Yy1*, *Bmp7-Ctgf* shRNA significantly decreased p-Smad2 further by ~ 60%, suggesting that profound inhibition of TGFβ/Smad signaling is responsible for suppressing *Lmna* DCM and cardiac fibrosis (Figure 4c). Immunostaining of macrophage marker Iba-1 showed infiltration of macrophages in *Lmna* DCM hearts (Figure 1f, 4d). The increased Iba-1 signal in *Lmna* DCM hearts was not significantly affected by *Bmp7* or *Ctgf* shRNA, suggesting that total macrophage numbers are not affected by *Bmp7* or *Ctgf*. On a simplified basis, macrophages may be polarized into two broad types, M1 (classically activated macrophages) and M2 (alternatively activated macrophages)[31]. The expression of M2 macrophages markers *Arg-1* and *Chil3* were induced more in *Lmna* DCM hearts treated with *Bmp7* compared to *Ctgf* shRNA (Figure 4e). However, the number of Arg-1 positive cells was not significantly increased in *Lmna* DCM hearts treated with *Bmp7* compared to *EGFP*, suggesting *Bmp7* has a limited role in regulating cardiac macrophage polarization (Figure 4f). Interestingly, CD3+ T cell numbers in *Lmna* DCM hearts were reduced by *Bmp7-Ctgf* shRNA, but not *Bmp7* or *Ctgf* shRNA individually (Figure 4g). Consistent with previous results, modulation of *Bmp7* or *Ctgf* alone is not sufficient to suppress DCM, cardiac fibrosis and inflammation. Taken together, these results suggest that modulation of both *Bmp7* and *Ctgf* suppresses DCM and cardiac fibrosis by inhibiting the TGFβ/Smad signaling pathway and regulating cardiac inflammation.

Discussion

Pathogenic variants in *LMNA* are common causes of familial DCM with penetrance exceeding 90%[32, 33]. *LMNA* insufficiency due to pathogenic missense or nonsense mutations is suggested as a causal mechanism. *Lmna* knockout mice (−/−) exhibited systemic defects in addition to DCM[6]. *Lmna* +/−heterozygote mice developed late onset of DCM, suggesting a dose dependent effect in *Lmna* related DCM[34]. In addition, DCM mice induced by mutated *Lmna* (nPLAO/nPLAO) was less severe compared to *Lmna* (nPLAO/-) DCM mice, suggesting that certain *LMNA* related DCM is caused by insufficient *LMNA*, rather than toxic mutant *LMNA*[35]. *LMNA* is expressed in most cell types including CMs and non-CMs in heart tissues. It was previously unclear whether CM specific silencing of *LMNA* is sufficient to induce DCM. Here, without multiple crossing of compound genetic modified mice or overexpression of Cre or tamoxifen administration, we generated a new DCM mouse model by silencing *Lmna* specifically in CMs. This *Lmna* model resulted in a typical DCM phenotype including enlarged LV, reduced LV wall thickness and markedly impaired systolic function. Our *Lmna* DCM model showed a significant increase of cardiac interstitial fibrosis accompanied by cardiac inflammation. By reducing *Lmna* expression specifically in CMs, we provide a new *Lmna* DCM model complementary to genetic models currently available to study *Lmna* related diseases.

We uncovered that upregulation of *Yy1* suppressed *Lmna* DCM and cardiac fibrosis by upregulating *Bmp7* and downregulating *Ctgf* gene expression. *Bmp7* was one important downstream target of *Yy1* in suppressing DCM and cardiac fibrosis in the *Lmna* DCM model. *Bmp7* is believed to suppress fibrosis by activating Smad1/5/8 and counteracting the TGFβ/Smad2/3 signaling pathway[36, 37]. TGFβ signaling is known to suppress cardiac *Bmp7* expression[24]. In addition, upregulation of *Bmp7* inhibits endothelial mesenchymal transition (EndMT) and cardiac fibrosis by opposing TGF-β signaling[38]. However, upregulation of *Bmp7* in our model was not sufficient to suppress *Lmna* DCM/cardiac fibrosis and upregulation of TGFβ/Smad signaling. Instead, TGFβ/Smad signaling was dramatically suppressed by co-modulation of *Bmp7* and *Ctgf*. *Lmna* DCM hearts showed infiltration of inflammatory cells including macrophages and T cells. Upregulation of *Bmp7* alone did not affect macrophage infiltration, macrophage polarization or T cell infiltration in *Lmna* DCM hearts. Consequently, Bmp7 did not suppress DCM and cardiac fibrosis. Recently, blocking of activated T cells was shown to prevent progressive left ventricular dilatation in myocardial infarction models[39, 40]. Therefore, the observed reduction of T cell infiltration following co-modulation of *Bmp7* and *Ctgf* may also play a role in attenuating *Lmna* DCM.

Ctgf is a known downstream gene of the TGFβ signaling pathway and is highly induced in various cardiovascular diseases[28]. Ctgf is believed to be a pro-fibrotic factor in many organs including the heart[29]. In our model, silencing of *Ctgf* reduced p-Smad2, indicating a positive feed backup loop between *Ctgf* and the TGFβ/Smad signaling pathway. Again, silencing of *Ctgf* alone did not significantly suppress *Lmna* DCM and cardiac fibrosis or inflammation. Thus, modulating individual downstream targets of the *Yy1* gene may be insufficient to recapitulate its suppressive role in *Lmna* DCM. We reveal that *Yy1* indeed played a yin yang role in transcriptional regulation of *Bmp7* and *Ctgf*, reflecting its capacity as either an activator or repressor in gene regulation[41]. Importantly, we reveal that *Bmp7* and *Ctgf*

control multiple key modalities of *Lmna* DCM pathology, suggesting that combination treatment may be beneficial to individuals with *Lmna* DCM and possibly other cardiomyopathies.

AAV is a relatively safe, and increasingly used delivery tool for gene therapy[42]. *Bmp7* delivered by AAV could overcome issues with the relatively short half-life of Bmp7 by intravenous or intraperitoneal administration[43]. Silencing of *Ctgf* by shRNA also represents an alternative to anti-CTGF antibodies which have been shown to improve outcomes in animal models of fibrotic disease[44]. Indeed, an anti-CTGF antibody is under evaluation in a clinical trial for treatment of idiopathic pulmonary fibrosis (IPF)[45]. It will be of great interest to know whether anti-CTGF works together with *Bmp7* to suppress *Lmna* DCM and cardiac fibrosis. Taken together, our findings provide substantial supporting data for translational research to treat *LMNA* related DCM.

Supplementary Material

Refer to Web version on PubMed Central for supplementary material.

Acknowledgments

We thank Ms. Zenia Tiang (Genome Institute of Singapore, Singapore) for RNAseq technical assistance. We thank Dr. Kenji Onoue (Nara Medical University, Japan) and Dr. Mark Richards (NUHS, Singapore) for discussion and comments on the manuscript.

Sources Of Funding

This work was supported by grants from NMRC (J. J, R.F, NMRC/CIRG/1431/2015, NMRC/OFIRG/0056/2017 and J.W.W, NMRC/OFYIRG/0081/2018), MOE T1 (J.J, NUHS O-CRG 2016 and J.W.W NUHS O-CRG 2016 Oct-23) and Startup (NUHS J.J)

Nonstandard Abbreviations and Acronyms:

αSMA	α-smooth muscle actin
AAV	Adeno-associated virus
Bmp7	Bone morphogenetic protein 7
Ccnd1	Cyclin D1
Ctgf	Connective tissue growth factor
CM	Cardiomyocytes
DCM	Dilated cardiomyopathy
ECM	Extracellular matrix
shRNA	Short hairpin RNA
Lmna	Lamin A/C
Myh7	Myosin heavy chain 7

Nppa	Natriuretic peptide A
PCM1	Pericentriolar material 1
Postn	Periostin
Tgfβ	Transforming growth factor beta
Yy1	Yin Yang 1

References

1. Weintraub RG, Semsarian C, Macdonald P. Dilated cardiomyopathy. Lancet. 2017;390:400–414 [PubMed: 28190577]
2. Hershberger RE, Hedges DJ, Morales A. Dilated cardiomyopathy: The complexity of a diverse genetic architecture. Nat Rev Cardiol. 2013;10:531–547 [PubMed: 23900355]
3. McNally EM, Golbus JR, Puckelwartz MJ. Genetic mutations and mechanisms in dilated cardiomyopathy. J Clin Invest. 2013;123:19–26 [PubMed: 23281406]
4. Lu JT, Muchir A, Nagy PL, Worman HJ. Lmna cardiomyopathy: Cell biology and genetics meet clinical medicine. Dis Model Mech. 2011;4:562–568 [PubMed: 21810905]
5. Sullivan T, Escalante-Alcalde D, Bhatt H, Anver M, Bhat N, Nagashima K, Stewart CL, Burke B. Loss of a-type lamin expression compromises nuclear envelope integrity leading to muscular dystrophy. J Cell Biol. 1999;147:913–920 [PubMed: 10579712]
6. Nikolova V, Leimena C, McMahon AC, Tan JC, Chandar S, Jogia D, Kesteven SH, Michalicek J, Otway R, Verheyen F, Rainer S, Stewart CL, Martin D, Feneley MP, Fatkin D. Defects in nuclear structure and function promote dilated cardiomyopathy in lamin a/c-deficient mice. J Clin Invest. 2004;113:357–369 [PubMed: 14755333]
7. Kubben N, Voncken JW, Konings G, van Weeghel M, van den Hoogenhof MM, Gijbels M, van Erk A, Schoonderwoerd K, van den Bosch B, Dahlmans V, Calis C, Houten SM, Misteli T, Pinto YM. Post-natal myogenic and adipogenic developmental: Defects and metabolic impairment upon loss of a-type lamins. Nucleus. 2011;2:195–207 [PubMed: 21818413]
8. Choi JC, Muchir A, Wu W, Iwata S, Homma S, Morrow JP, Worman HJ. Temsirolimus activates autophagy and ameliorates cardiomyopathy caused by lamin a/c gene mutation. Sci Transl Med. 2012;4:144ra102
9. Liao CY, Anderson SS, Chicoine NH, Mayfield JR, Academia EC, Wilson JA, Pongkietisak C, Thompson MA, Lagmay EP, Miller DM, Hsu YM, McCormick MA, O'Leary MN, Kennedy BK. Rapamycin reverses metabolic deficits in lamin a/c-deficient mice. Cell Rep. 2016;17:2542–2552 [PubMed: 27926859]
10. Muchir A, Pavlidis P, Decostre V, Herron AJ, Arimura T, Bonne G, Worman HJ. Activation of mapk pathways links lmna mutations to cardiomyopathy in emery-dreifuss muscular dystrophy. J Clin Invest. 2007;117:1282–1293 [PubMed: 17446932]
11. Le Dour C, Macquart C, Sera F, Homma S, Bonne G, Morrow JP, Worman HJ, Muchir A. Decreased wnt/beta-catenin signalling contributes to the pathogenesis of dilated cardiomyopathy caused by mutations in the lamin a/c gene. Hum Mol Genet. 2017;26:333–343 [PubMed: 28069793]
12. Osorio FG, Barcena C, Soria-Valles C, Ramsay AJ, de Carlos F, Cobo J, Fueyo A, Freije JM, Lopez-Otin C. Nuclear lamina defects cause atm-dependent nf-kappab activation and link accelerated aging to a systemic inflammatory response. Genes Dev. 2012;26:2311–2324 [PubMed: 23019125]
13. Muchir A, Wu W, Choi JC, Iwata S, Morrow J, Homma S, Worman HJ. Abnormal p38alpha mitogen-activated protein kinase signaling in dilated cardiomyopathy caused by lamin a/c gene mutation. Hum Mol Genet. 2012;21:4325–4333 [PubMed: 22773734]

14. Jiang J, Wakimoto H, Seidman JG, Seidman CE. Allele-specific silencing of mutant myh6 transcripts in mice suppresses hypertrophic cardiomyopathy. Science. 2013;342:111–114 [PubMed: 24092743]
15. Jiang J, Burgon PG, Wakimoto H, Onoue K, Gorham JM, O'Meara CC, Fomovsky G, McConnell BK, Lee RT, Seidman JG, Seidman CE. Cardiac myosin binding protein c regulates postnatal myocyte cytokinesis. Proc Natl Acad Sci U S A. 2015;112:9046–9051 [PubMed: 26153423]
16. Bersell K, Choudhury S, Mollova M, Polizzotti BD, Ganapathy B, Walsh S, Wadugu B, Arab S, Kuhn B. Moderate and high amounts of tamoxifen in alphamhc-mercremer mice induce a DNA damage response, leading to heart failure and death. Dis Model Mech. 2013;6:1459–1469 [PubMed: 23929941]
17. Cheedipudi SM, Matkovich SJ, Coarfa C, Hu X, Robertson MJ, Sweet M, Taylor M, Mestroni L, Cleveland J, Willerson JT, Gurha P, Marian AJ. Genomic reorganization of lamin-associated domains in cardiac myocytes is associated with differential gene expression and DNA methylation in human dilated cardiomyopathy. Circ Res. 2019;124:1198–1213 [PubMed: 30739589]
18. Chen SN, Lombardi R, Karmouch J, Tsai JY, Czernuszewicz G, Taylor MRG, Mestroni L, Coarfa C, Gurha P, Marian AJ. DNA damage response/tp53 pathway is activated and contributes to the pathogenesis of dilated cardiomyopathy associated with lmna (lamin a/c) mutations. Circ Res. 2019;124:856–873 [PubMed: 30696354]
19. Gordon S, Akopyan G, Garban H, Bonavida B. Transcription factor yy1: Structure, function, and therapeutic implications in cancer biology. Oncogene. 2006;25:1125–1142 [PubMed: 16314846]
20. Cicatiello L, Addeo R, Sasso A, Altucci L, Petrizzi VB, Borgo R, Cancemi M, Caporali S, Caristi S, Scafoglio C, Teti D, Bresciani F, Perillo B, Weisz A. Estrogens and progesterone promote persistent ccnd1 gene activation during g1 by inducing transcriptional derepression via c-jun/cfos/estrogen receptor (progesterone receptor) complex assembly to a distal regulatory element and recruitment of cyclin d1 to its own gene promoter. Mol Cell Biol. 2004;24:7260–7274 [PubMed: 15282324]
21. Dobaczewski M, Chen W, Frangogiannis NG. Transforming growth factor (tgf)-beta signaling in cardiac remodeling. J Mol Cell Cardiol. 2011;51:600–606 [PubMed: 21059352]
22. Chen MM, Lam A, Abraham JA, Schreiner GF, Joly AH. Ctgf expression is induced by tgf- beta in cardiac fibroblasts and cardiac myocytes: A potential role in heart fibrosis. J Mol Cell Cardiol. 2000;32:1805–1819 [PubMed: 11013125]
23. Zhao S, Wu H, Xia W, Chen X, Zhu S, Zhang S, Shao Y, Ma W, Yang D, Zhang J. Periostin expression is upregulated and associated with myocardial fibrosis in human failing hearts. J Cardiol. 2014;63:373–378 [PubMed: 24219836]
24. Koitabashi N, Danner T, Zaiman AL, Pinto YM, Rowell J, Mankowski J, Zhang D, Nakamura T, Takimoto E, Kass DA. Pivotal role of cardiomyocyte tgf-beta signaling in the murine pathological response to sustained pressure overload. J Clin Invest. 2011;121:2301–2312 [PubMed: 21537080]
25. Merino D, Villar AV, Garcia R, Tramullas M, Ruiz L, Ribas C, Cabezudo S, Nistal JF, Hurle MA. Bmp-7 attenuates left ventricular remodelling under pressure overload and facilitates reverse remodelling and functional recovery. Cardiovasc Res. 2016;110:331–345 [PubMed: 27068510]
26. Zeisberg M, Hanai J, Sugimoto H, Mammoto T, Charytan D, Strutz F, Kalluri R. Bmp-7 counteracts tgf-beta1-induced epithelial-to-mesenchymal transition and reverses chronic renal injury. Nat Med. 2003;9:964–968 [PubMed: 12808448]
27. Yang G, Zhu Z, Wang Y, Gao A, Niu P, Tian L. Bone morphogenetic protein-7 inhibits silica-induced pulmonary fibrosis in rats. Toxicol Lett. 2013;220:103–108 [PubMed: 23639248]
28. Lipson KE, Wong C, Teng Y, Spong S. Ctgf is a central mediator of tissue remodeling and fibrosis and its inhibition can reverse the process of fibrosis. Fibrogenesis Tissue Repair. 2012;5:S24 [PubMed: 23259531]
29. Dorn LE, Petrosino JM, Wright P, Accornero F. Ctgf/ccn2 is an autocrine regulator of cardiac fibrosis. J Mol Cell Cardiol. 2018;121:205–211 [PubMed: 30040954]
30. Ackers-Johnson M, Li PY, Holmes AP, O'Brien SM, Pavlovic D, Foo RS. A simplified, langendorff-free method for concomitant isolation of viable cardiac myocytes and nonmyocytes from the adult mouse heart. Circ Res. 2016;119:909–920 [PubMed: 27502479]

31. Mantovani A, Sozzani S, Locati M, Allavena P, Sica A. Macrophage polarization: Tumor-associated macrophages as a paradigm for polarized m2 mononuclear phagocytes. Trends Immunol. 2002;23:549–555 [PubMed: 12401408]
32. Pasotti M, Klersy C, Pilotto A, Marziliano N, Rapezzi C, Serio A, Mannarino S, Gambarin F, Favalli V, Grasso M, Agozzino M, Campana C, Gavazzi A, Febo O, Marini M, Landolina M, Mortara A, Piccolo G, Vigano M, Tavazzi L, Arbustini E. Long-term outcome and risk stratification in dilated cardiolaminopathies. J Am Coll Cardiol. 2008;52:1250–1260 [PubMed: 18926329]
33. van Berlo JH, de Voogt WG, van der Kooi AJ, van Tintelen JP, Bonne G, Yaou RB, Duboc D, Rossenbacker T, Heidbuchel H, de Visser M, Crijns HJ, Pinto YM. Meta-analysis of clinical characteristics of 299 carriers of lmna gene mutations: Do lamin a/c mutations portend a high risk of sudden death? J Mol Med (Berl). 2005;83:79–83 [PubMed: 15551023]
34. Wolf CM, Wang L, Alcalai R, Pizard A, Burgon PG, Ahmad F, Sherwood M, Branco DM, Wakimoto H, Fishman GI, See V, Stewart CL, Conner DA, Berul CI, Seidman CE, Seidman JG. Lamin a/c haploinsufficiency causes dilated cardiomyopathy and apoptosis-triggered cardiac conduction system disease. J Mol Cell Cardiol. 2008;44:293–303 [PubMed: 18182166]
35. Davies BS, Barnes RH 2nd, Tu Y, Ren S, Andres DA, Spielmann HP, Lammerding J, Wang Y, Young SG, Fong LG. An accumulation of non-farnesylated prelamin a causes cardiomyopathy but not progeria. Hum Mol Genet. 2010;19:2682–2694 [PubMed: 20421363]
36. Meng XM, Chung AC, Lan HY. Role of the tgf-beta/bmp-7/smad pathways in renal diseases. Clin Sci (Lond). 2013;124:243–254 [PubMed: 23126427]
37. Flevaris P, Khan SS, Eren M, Schuldt AJT, Shah SJ, Lee DC, Gupta S, Shapiro AD, Burridge PW, Ghosh AK, Vaughan DE. Plasminogen activator inhibitor type i controls cardiomyocyte transforming growth factor-beta and cardiac fibrosis. Circulation. 2017;136:664–679 [PubMed: 28588076]
38. Zeisberg EM, Tarnavski O, Zeisberg M, Dorfman AL, McMullen JR, Gustafsson E, Chandraker A, Yuan X, Pu WT, Roberts AB, Neilson EG, Sayegh MH, Izumo S, Kalluri R. Endothelial-tomesenchymal transition contributes to cardiac fibrosis. Nat Med. 2007;13:952–961 [PubMed: 17660828]
39. Laroumanie F, Douin-Echinard V, Pozzo J, Lairez O, Tortosa F, Vinel C, Delage C, Calise D, Dutaur M, Parini A, Pizzinat N. Cd4+ t cells promote the transition from hypertrophy to heart failure during chronic pressure overload. Circulation. 2014;129:2111–2124 [PubMed: 24657994]
40. Bansal SS, Ismahil MA, Goel M, Patel B, Hamid T, Rokosh G, Prabhu SD. Activated t lymphocytes are essential drivers of pathological remodeling in ischemic heart failure. Circ Heart Fail. 2017;10:e003688 [PubMed: 28242779]
41. Deng Z, Cao P, Wan MM, Sui G. Yin yang 1: A multifaceted protein beyond a transcription factor. Transcription. 2010;1:81–84 [PubMed: 21326896]
42. Dunbar CE, High KA, Joung JK, Kohn DB, Ozawa K, Sadelain M. Gene therapy comes of age. Science. 2018;359 [PubMed: 29700239]
43. Vukicevic S, Basic V, Rogic D, Basic N, Shih MS, Shepard A, Jin D, Dattatreyamurty B, Jones W, Dorai H, Ryan S, Griffiths D, Maliakal J, Jelic M, Pastorcic M, Stavljenic A, Sampath TK. Osteogenic protein-1 (bone morphogenetic protein-7) reduces severity of injury after ischemic acute renal failure in rat. J Clin Invest. 1998;102:202–214 [PubMed: 9649574]
44. Wang Q, Usinger W, Nichols B, Gray J, Xu L, Seeley TW, Brenner M, Guo G, Zhang W, Oliver N, Lin A, Yeowell D. Cooperative interaction of ctgf and tgf-beta in animal models of fibrotic disease. Fibrogenesis Tissue Repair. 2011;4:4 [PubMed: 21284856]
45. Raghu G, Scholand MB, de Andrade J, Lancaster L, Mageto Y, Goldin J, Brown KK, Flaherty KR, Wencel M, Wanger J, Neff T, Valone F, Stauffer J, Porter S. Fg-3019 anti-connective tissue growth factor monoclonal antibody: Results of an open-label clinical trial in idiopathic pulmonary fibrosis. Eur Respir J. 2016;47:1481–1491 [PubMed: 26965296]

NOVELTY AND SIGNIFICANCE

What Is Known?

- *LMNA* mutations causes many defects including DCM.
- *Lmna* knockout mice exhibit systemic defects in addition to DCM

What New Information Does This Article Contribute?

- Cardiac *Lmna* insufficiency causes DCM coupled with cardiac fibrosis.
- Upregulation of *Yy1* suppresses *Lmna* DCM and cardiac fibrosis independent of cardiac cell cycle regulation.
- *Yy1* regulates its downstream targets *Bmp7* and *Ctgf*.
- *Bmp7* serves as an important downstream gene of *Yy1* in suppression of *Lmna* DCM and cardiac fibrosis.
- Simultaneous upregulation of *Bmp7* and suppression of *Ctgf* suppresses *Lmna* DCM and cardiac fibrosis.

LMNA mutants causes many defects including dilated cardiomyopathy (DCM). There is a lack of information on whether cardiac specific modulation of *LMNA* induces DCM. Herein, we reveal that reduction of cardiac *Lmna* causes DCM coupled with cardiac fibrosis in mice. Moreover, we demonstrate that upregulation of a transcription factor Yin Yang 1 (*Yy1*) suppresses *Lmna* DCM and cardiac fibrosis through regulation of its downstream genes, *Bmp7* and *Ctgf*. Interestingly, modulation of *Bmp7* or *Ctgf* individually was not sufficient to suppress DCM and cardiac fibrosis. Importantly, upregulation of *Bmp7* together with *Ctgf* silencing significantly suppressed DCM and cardiac fibrosis through inhibition of TGFβ/Smad signaling. Our findings uncover a novel role of *Yy1* and its downstream genes, and provide a solid foundation for the development of *Yy1*, *Bmp7* or *Ctgf* as therapeutic targets for DCM and cardiac fibrosis.

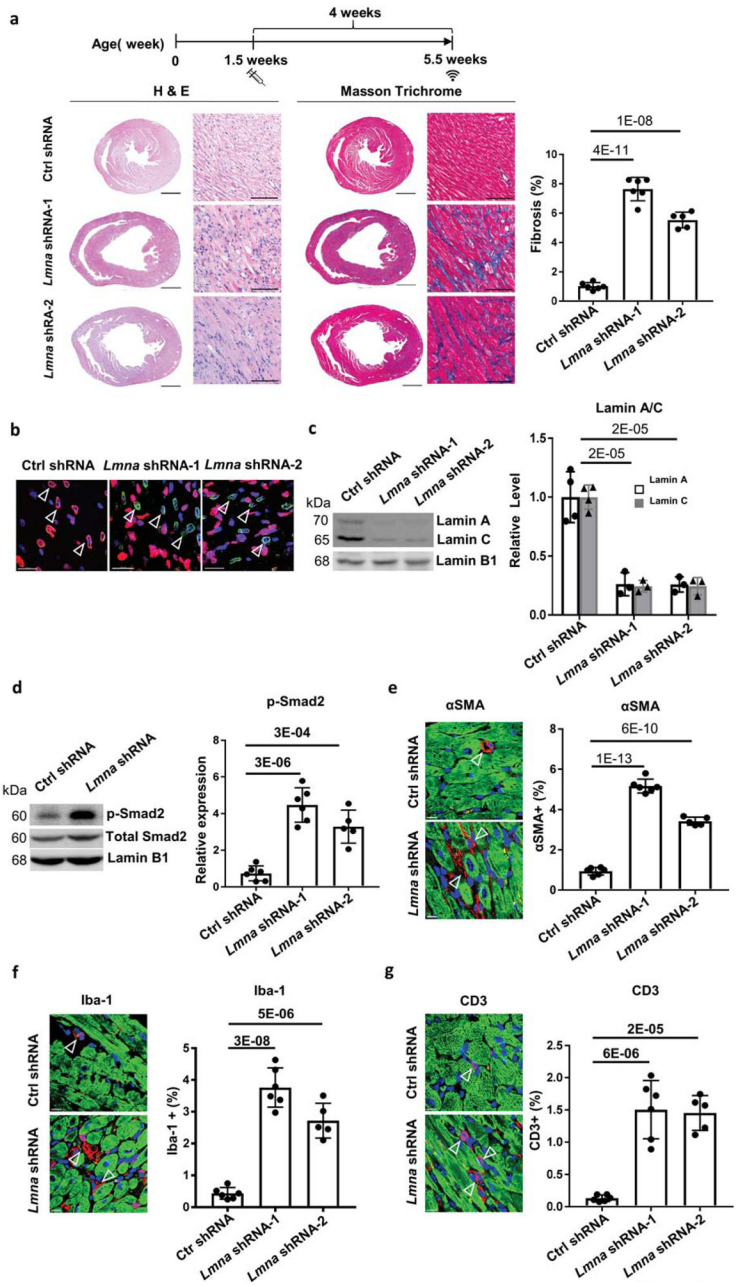

Figure 1. Cardiac specific *Lmna* shRNA induces DCM in mice.

(**a**) Experimental timeline showing timepoints of virus injection and echocardiogram. Cardiac performance was assessed by echocardiogram at 5.5 week old. H&E and Masson Trichrome (MT) staining was performed on paraffin heart sections taken 4 weeks after control shRNA and *Lmna* shRNA transduction. Quantification of myocardial fibrosis of MT sections is shown, virus dose, 2.0E+13 vg/kg, n ≥ 5. Scale bars: 1000 μm for complete heart images; 100 μm for enlarged images. (**b**) Paraffin heart section immunostained for Lamin A/C (red), PCM1 (green) and DAPI (blue) in mice transduced with control shRNA and *Lmna* shRNA, scale bar = 100 μm. (**c, d**) Western blot and quantitative analysis of Lamin A/C protein levels in isolated cardiomyocytes (**c**) and phospho-Smad2 protein levels in

mouse heart tissues (**d**), n ≥ 3. Data were normalized to Lamin B1. (**e-g**) Paraffin heart sections (left) and quantifications (right) of (**e**) αSMA (red), (**f**) Iba-1 (red) and (**g**) CD3 (red), cTnI (green) and DAPI (blue) positive cells in mice transduced with control shRNA (top) and *Lmna* shRNA (bottom), n ≥ 5, scale bar = 50 μm.

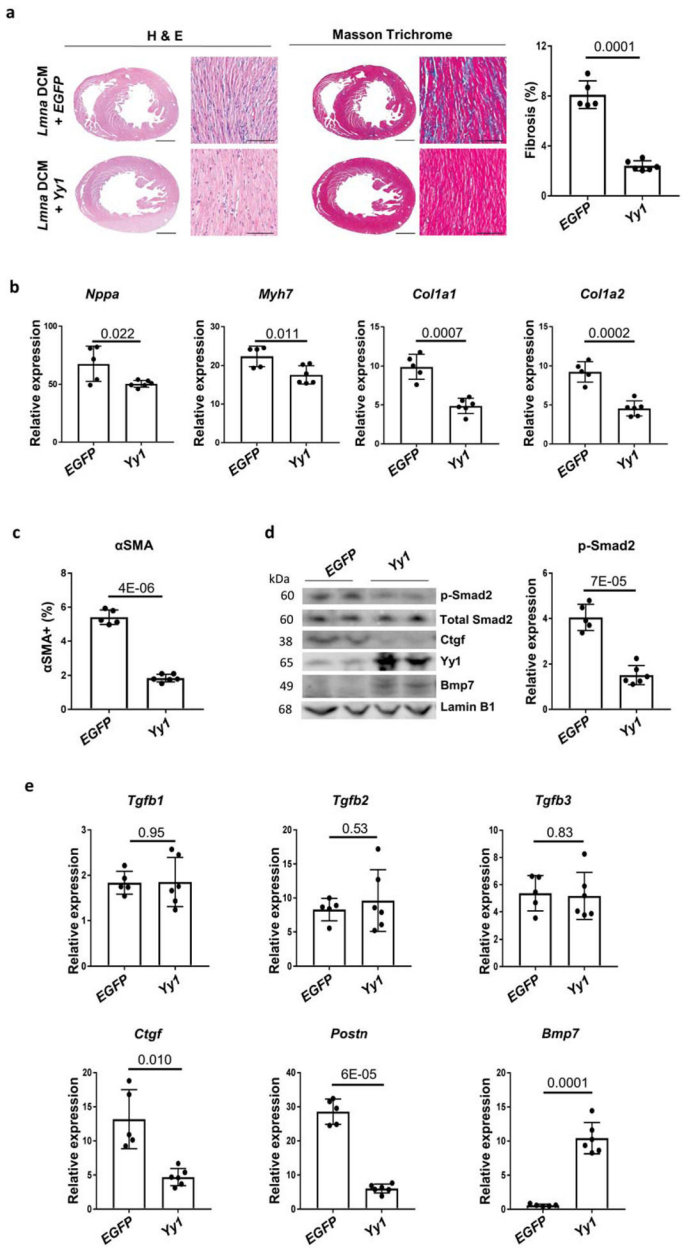

Figure 2. *Yy1* suppresses *Lmna* DCM and cardiac fibrosis

(**a**) H&E and MT staining of paraffin heart sections of *Lmna* DCM mice treated with *EGFP* or *Yy1*. Quantification of myocardial fibrosis of MT sections is shown, n ≥ 5. Scale bars: 1000 μm for complete heart images; 100 μm for enlarged images. (**b**) Quantitative real-time PCR analyses of *Nppa*, *Myh7*, *Col1a1* and *Col1a2* expressions in *EGFP* and *Yy1* treated groups. Mouse hearts were harvested 4 weeks after transduction, n ≥ 5. (**c**) Quantification of αSMA positive cells in paraffin heart sections from *Lmna* DCM mice treated with *EGFP* and *Yy1*, n ≥ 5. (**d**) Western blot and quantitative analysis of phospho-Smad2 (p-Smad2) protein levels in mouse heart tissue of *Lmna* DCM mice treated with *EGFP* and *Yy1*, n ≥ 5. Data were normalized to Lamin B1. (**e**) Quantitative real-time PCR analyses of *Tgfb1*,

Tgfb2, *Tgfb3*, *Ctgf, Postn* and *Bmp7* in *Lmna* DCM mice treated with *EGFP* and *Yy1*, n ≥ 5.

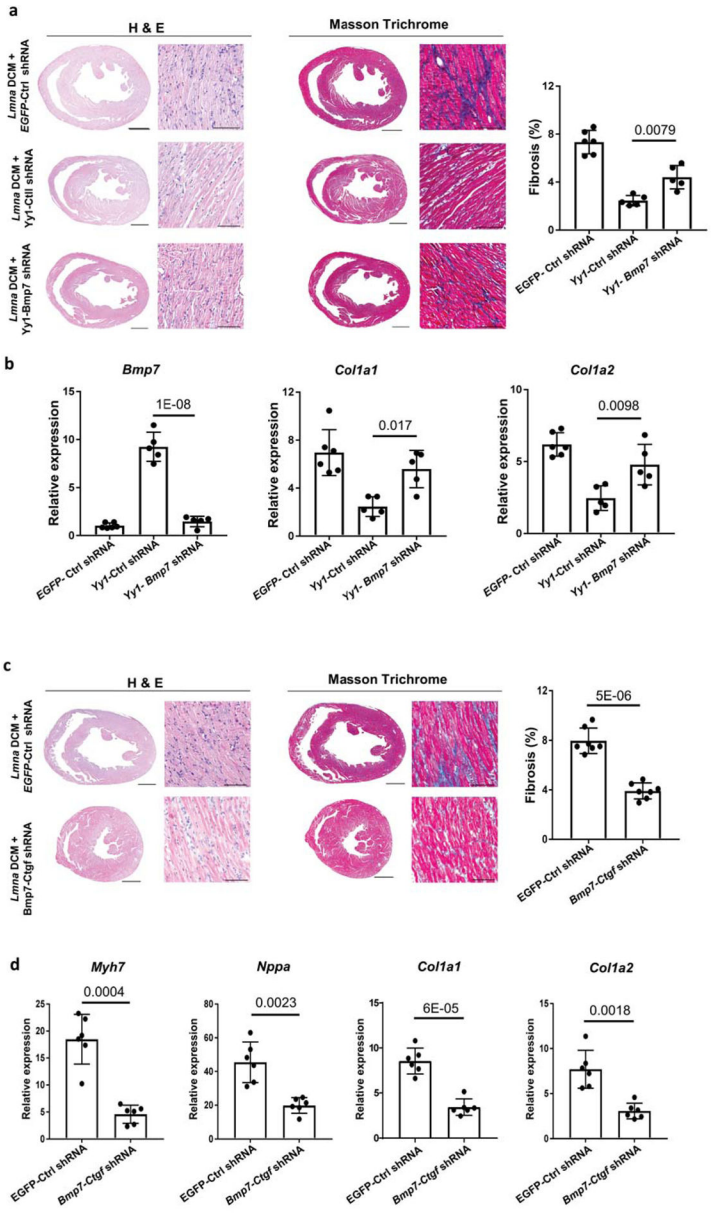

Figure 3. Co-regulation of *Bmp7* and *Ctgf* suppresses *Lmna* DCM and cardiac fibrosis

(**a** and **c**) H&E (left panel) and MT (middle panel) staining of paraffin heart sections of *Lmna* DCM mice 4 weeks after (**a**) *EGFP*-Ctrl shRNA, *Yy1*-Ctrl shRNA or *Yy1-Bmp7* shRNA transduction and (**c**) *EGFP*-Ctrl shRNA or *Bmp7-Ctgf* shRNA transduction. Quantification of myocardial fibrosis (right panel) from MT-stained sections, n ≥ 6. Scale bars: 1000 μm for complete heart images; 100 μm for enlarged images. (**b**) Quantitative real-time PCR analyses of *Bmp7*, *Col1a1* and *Col1a2* expression in *Lmna* DCM groups treated with *EGFP*-Ctrl shRNA, *Yy1*-Ctrl shRNA or *Yy1-Bmp7* shRNA, n ≥ 5. **(d)** Quantitative real-time PCR analyses of *Myh7*, *Nppa*, *Col1a1* and *Col1a2* expressions in *Lmna* DCM groups treated with *EGFP*-Ctrl shRNA or *Bmp7-Ctgf* shRNA groups, n ≥ 6.

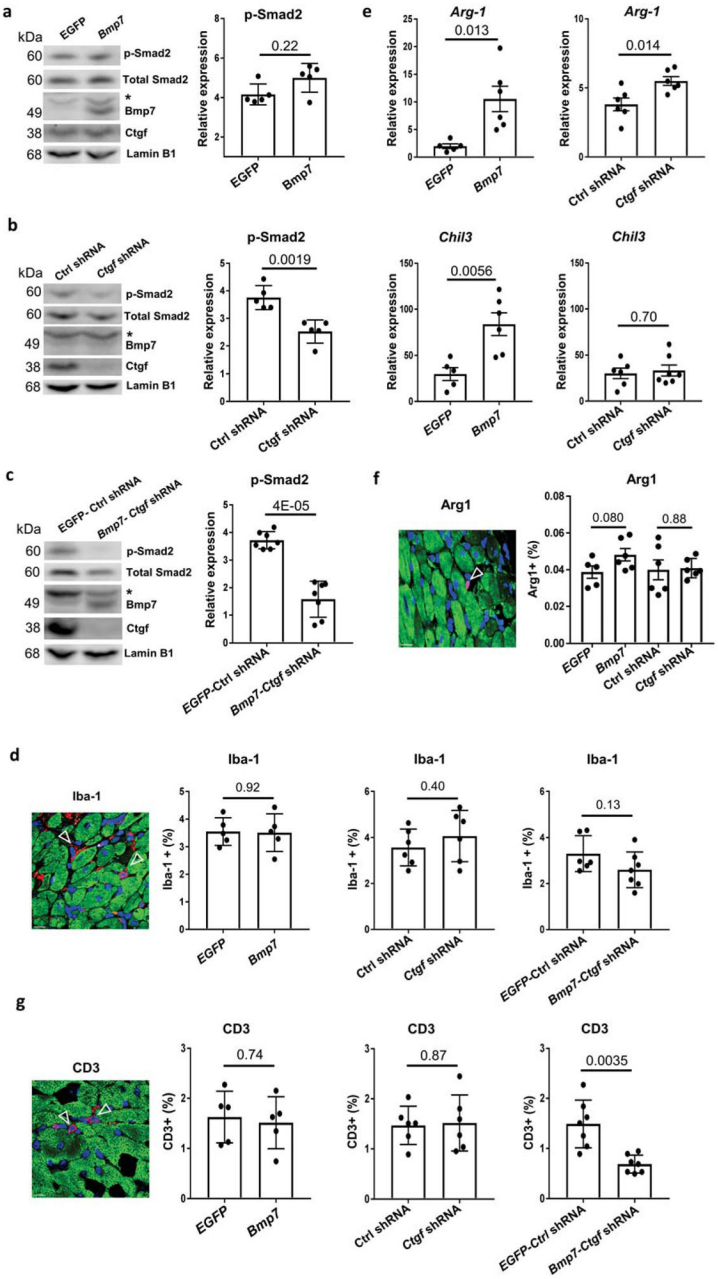

Figure 4. *Bmp7* and *Ctgf* regulate cardiac inflammation and TGFβ signaling

(**a-c**) Western blot (left panel) and quantitative analysis (right panel) of phospho-Smad2 (p-Smad2) protein levels in mouse heart tissue of *Lmna* DCM groups treated with (**a**) *EGFP* or *Bmp7*; (**b**) *Ctrl* shRNA or *Ctgf* shRNA or (**c**) *EGFP* Ctrl shRNA or *Bmp7-Ctgf* shRNA, n ≥ 5. Data were normalized to Lamin B1.* indicates the non-specific band. (**d**, **f** and **g**) Paraffin heart section staining (left panel) and quantifications (right pane) of (**d**) Iba-1 (red), (**f**) Arginase 1 (red) and (**g**) CD3 (red), cTnI (green) and DAPI (blue) positive cells in *Lmna* DCM groups treated with *EGFP*, *Bmp7*, *Ctrl* shRNA, *Ctgf* shRNA, *EGFP*-Ctrl shRNA or *Bmp7-Ctgf* shRNA, scale bar = 50 μm, n ≥5. (**e)** Quantitative real-time PCR analyses of

Arg-1 and *Chl3* expression in *Lmna* DCM groups treated with *EGFP*, *Bmp7*, *Ctrl* shRNA, *Ctgf* shRNA, n ≥ 5.

Table 1.

Effect of *Lmna* shRNA on cardiac function in mice.

Effect of *Lmna* shRNA-1 and *Lmna* shRNA-2 versus Ctrl shRNA on mice at a dose of 2.0E+13 vg/kg assessed at 5.5 weeks. P values represent comparisons to mice transduced with control shRNA at respective age. LVDD, left ventricular diastolic dimension; LVWT, LV wall thickness; EF, ejection fraction; FS, fractional shortening.

shRNA	Age (weeks)	n	LVDD (mm)	P	LVWT (mm)	P	EF (%)	P	FS (%)	P
Ctrl shRNA	5.5	6	3.81 ± 0.10		0.68 ± 0.10		57.80 ± 4.81		29.97 ± 3.20	
Lmna shRNA-1		6	4.25 ± 0.11	2E-06	0.45 ± 0.08	2E-05	12.13 ± 3.16	4E-11	5.33 ± 1.79	8E-11
Lmna shRNA-2		5	4.30 ± 0.32	5E-04	0.43 ± 0.12	4E-03	11.66 ± 10.66	1E-05	5.42 ± 5.01	1E-05

Table 2.

Effect of *Yy1* on *Lmna* DCM in mice

Effect of *Yy1* or *EGFP* at a dose of 0.5E+13 vg/kg on *Lmna* DCM mice assessed at 5.5 weeks. P values represent comparisons to *Lmna* DCM mice treated with *EGFP*. LVDD, left ventricular diastolic dimension; LVWT, LV wall thickness; EF, ejection fraction; FS, fractional shortening.

***Lmna* DCM Treatment**	**Age (weeks)**	**n**	**LVDD (mm)**	**P**	**LVWT (mm)**	**P**	**EF (%)**	**P**	**FS (%)**	**P**
EGFP	5.5	5	4.23 ± 0.10		0.40 ± 0.07		14.98 ± 4.39		6.64 ± 2.03	
Yy1		6	3.97 ± 0.18	0.02	0.51 ± 0.06	0.03	27.40 ± 2.55	0.0002	12.54 ± 1.27	0.0002

Table 3.

Effect of *Yy1-Bmp7* shRNA on Lmna DCM in mice

Effect of *Yy1-Bmp7* shRNA, *Yy1*-Ctrl shRNA or *EGFP*-Ctrl shRNA at a dose of 0.5E+13 vg/kg on *Lmna* DCM assessed at 5.5 weeks. P values represent comparisons to *Lmna* DCM mice treated with *EGFP*-Ctrl shRNA. LVDD, left ventricular diastolic dimension; LVWT, LV wall thickness; EF, ejection fraction; FS, fractional shortening.

***Lmna* DCM Treatment**	**Age (weeks)**	**n**	**LVDD (mm)**	**P**	**LVWT (mm)**	**P**	**EF (%)**	**P**	**FS (%)**	**P**
EGFP-Ctrl *shRNA*	5.5	7	4.34 ± 0.17		0.41 ± 0.05		13.55 ±3.53		5.99 ± 1.63	
Yy1-Ctrl *shRNA*		8	4.09 ± 0.13	0.005	0.48 ± 0.06	0.03	28.98 ± 3.66	6E-07	13.38 ± 1.89	1E-06
Yy1-Bmp7 shRNA		8	4.58 ± 0.17	0.02	0.51 ± 0.07	0.01	14.07 ±2.78	0.76	6.25 ± 1.29	0.74

Table 4.
Effect of *Bmp7-Ctgf* shRNA on *Lmna* DCM in mice

Effect of *Bmp7-Ctgf* shRNA at a dose of 2.0E+13 vg/kg on *Lmna* DCM mice assessed at 5.5 weeks. values represent comparisons to *Lmna* DCM mice treated with *EGFP*-Ctrl shRNA. LVDD, left ventricular diastolic dimension; LVWT, LV wall thickness; EF, ejection fraction; FS, fractional shortening.

***Lmna* DCM Treatment**	**Age (weeks)**	**n**		**LVDD (mm)**	**P**	**LVWT (mm)**	**P**	**EF (%)**	**P**	**FS (%)**	**P**
EGFP-Ctrl shRNA	5.5	7		4.25 ± 0.15		0.44 ±0.09		14.31 ± 4.43		6.34 ± 2.04	
Bmp7-Ctgf shRNA		7		3.72 ± 0.06	2E-06	0.61 ±0.07	0.003	46.05 ± 4.89	2E-08	22.43 ± 2.62	2E-08